A new protocol to accurately track long–term orthodontic tooth movement and support patient-specific numerical modeling

Gauthier Dot, Raphael Licha, Florent Goussard, Vittorio Sansalone

Version of Record: https://www.sciencedirect.com/science/article/pii/S0021929021005261
Manuscript_5d53aed6a9e41a9ea8f19cb8a40ea53c

A new protocol to accurately track long-term orthodontic tooth movement and support patient-specific numerical modeling

Revision 2

Original Article

Gauthier DOT[1,2,3], Raphael LICHA[1,2], Florent GOUSSARD[4], Vittorio SANSALONE[1,2]

[1] Univ Paris Est Creteil, CNRS, MSME, F-94010 Creteil, France

[2] Univ Gustave Eiffel, MSME, F-77474 Marne-la-Vallée, France

[3] Service d'Odontologie, Hopital Pitie-Salpetriere, AP–HP, Universite de Paris, Paris, France

[4] CR2P, UMR 7207, Muséum national d'Histoire naturelle, CNRS, Sorbonne Université, 8 rue Buffon CP38 75005 Paris, France

Correspondence:

Vittorio SANSALONE

Univ Paris Est Creteil, CNRS, MSME, F-94010 Creteil, France

vittorio.sansalone@u-pec.fr

+33 6 28 06 85 65

Keywords : Tooth Movement ; Dental Models ; Cone-Beam Computed Tomography ; Finite Element Analyses

Word count (Introduction through Discussion) : 4000 words

A new protocol to accurately track long-term orthodontic tooth movement and support patient-specific numerical modeling

ABSTRACT (183 words)

Numerical simulation of long-term orthodontic tooth movement based on Finite Element Analysis (FEA) could help clinicians to plan more efficient and mechanically sound treatments. However, most of FEA studies assume idealized loading conditions and lack experimental calibration or validation. The goal of this paper is to propose a novel clinical protocol to accurately track orthodontic tooth displacement in three-dimensions (3D) and provide 3D models that may support FEA. Our protocol uses an initial cone beam computed tomography (CBCT) scan and several intra-oral scans (IOS) to generate 3D models of the maxillary bone and teeth ready for use in FEA. The protocol was applied to monitor the canine retraction of a patient during seven months. A second CBCT scan was performed at the end of the study for validation purposes. In order to ease FEA, a frictionless and statically determinate lingual device for maxillary canine retraction was designed. Numerical simulations were set up using the 3D models provided by our protocol to show the relevance of our proposal. Comparison of numerical and clinical results highlights the suitability of this protocol to support patient-specific FEA.

1. INTRODUCTION

Orthodontic treatments usually rely on an orthodontic archwire passing through braces bonded on the teeth, which can be associated to accessory elements like elastic chains or springs. Orthodontic forces transmitted to the teeth are related to the elastic deformation of these materials and to the friction and sliding of the archwire in the braces. These forces trigger alveolar bone remodeling and lead to orthodontic tooth movement (OTM) (Henneman et al., 2008; Krishnan and Davidovitch, 2009; Wise and King, 2008). Nowadays, orthodontic treatment strategies are primarily based on orthodontists' clinical experience. In some cases, unwanted effects may appear like orthodontic external root resorption (OERR) (Viecilli et al., 2013; Zhong et al., 2019) or difficulties in planning and predicting tooth movement might arise (Burstone, 2015).

Modeling and simulation have a great potential to support clinical activity (Likitmongkolsakul et al., 2018). In solid mechanics, Finite Element Analysis (FEA) is one of the most attractive numerical approaches. Recent advances in imaging techniques allow the set-up of image-based, patient-specific FEA whose relevance is largely acknowledged in several clinical domains. However, numerical simulation of long-term (several weeks or months) OTM remains a challenge despite the wealth of works existing on this subject (Table 1) (Bourauel et al., 2000; Chen et al., 2014; Hamanaka et al., 2017; Hasegawa et al., 2016; Likitmongkolsakul et al., 2018; Marangalou et al., 2009; Schneider et al., 2002; Wang et al., 2014).

A critical issue in the development of FEA of long-term OTM concerns the availability of suitable clinical data. Most of the existing works based on FEA showed no experimental calibration or validation. To the best of our knowledge, only two studies compared their numerical results with clinical data of one and two patients, respectively (Table 1) (Chen et al., 2014; Likitmongkolsakul et al., 2018). Numerical models cannot trustfully support clinical

practice as long as they are not properly validated against experimental data (Albogha and Takahashi, 2015; Hannam, 2011). In order to generate accurate three-dimensional (3D) patient-specific models of craniofacial structures, the main imaging techniques that may be used are Computed-Tomography (CT) and Cone Beam CT (CBCT) (Table 1). Due to its broad accessibility and low-dosimetry protocols, CBCT is more commonly used in orthodontics procedures (Kapila and Nervina, 2015). Although CBCT cannot be regarded as a standard method of diagnosis, its use can be justified for carefully designed research purposes (Kapila and Nervina, 2015). As with any radiographic examination, the three basic principles of radiation protection (justification, optimization and limitation) must be strictly observed, and CBCT scans cannot be repetitiously used to track OTM all along an orthodontic treatment. As shown in Table 1, only one published study tracked clinical OTM in order to update its model geometry, using scanned dental models (Likitmongkolsakul et al., 2018).

Furthermore, modeling assumptions, including loading conditions and material behavior, are key in order to set up reliable FEA. Accurate modeling of clinically realistic force systems is a major challenge of orthodontic simulations (George et al., 2019; Roberts et al., 2015). For example, friction and sliding of the archwire is very rarely considered, even in situations where it can have a major clinical impact (Table 1) (Hamanaka et al., 2017). The friction between the archwire and the braces can be hardly measured *in vivo* and therefore prevents an accurate calibration of patient-specific biomechanical models (George et al., 2019). More generally, a proper definition of the boundary conditions is a critical issue as long as the orthodontic forces are statically indeterminate as it is usually the case with traditional orthodontic treatments. Additionally, an inaccurate description of the orthodontic forces entails issues in the calibration of the constitutive models of the materials making up the maxillary structures. Indeed, an accurate knowledge of the prevailing mechanical forces and of the stress-strain distribution in the maxillary structures is required to understand the mechanical response and to calibrate suitable constitutive models for these materials. Thus,

coarse approximations on the description of the orthodontic forces can seriously threaten the reliability of the numerical simulations.

The main goal of this paper is to propose a new tracking protocol to generate 3D models of the maxillary system (bone and teeth) that can be used to set up and validate numerical models. It relies on one initial CBCT scan and monthly intra-oral scans (IOS). The frequency of IOS corresponds to the typical frequency of appointments in orthodontic practice. We tested the relevance of our proposal in a clinical situation, and used the 3D models to develop preliminary FE models (FEM) of the relevant maxillary structures. In order to reduce the bias in modeling the orthodontic forces, a frictionless and statically determinate lingual device for maxillary canine retraction was designed. Material parameters of the FEM were matched against clinical data.

2. MATERIALS AND METHODS

2.1. Clinical procedure

After verbal and written information about the research, one patient accepted to be included in the study. This 28-year-old patient showed a class I malocclusion, with significant anterior crowding and protrusion of incisors. The orthodontic treatment plan aimed at correcting the malocclusion with avulsion of upper and lower first premolars, recoil of the canines and repositioning of the incisors with controlled posterior anchorage loss. In the maxilla, after the avulsion of the upper first premolars, three Temporary Anchorage Devices (TADs) and a personalized lingual device were placed (Figure 1). This device was designed so as to apply a statically determinate system of orthodontic forces at the theoretical initial center of resistance of the canines—the point that a force should pass through in order to obtain a pure translation of the tooth. Details about the clinical procedure are given in the Supplementary Materials, Section A. This study was approved by the ethical committee of protection of persons (CPP Paris Ile-de-France 1, reference 2016-dec.14420 ND).

2.2. Data acquisition

A CBCT scan of the maxilla was acquired before the placement of the TADs using NewTom VGi EVO (NewTom, Verona, Italy) set at 110 kV, 6.9 mA, exposure time of 4.3 seconds, 12 x 8 cm field of view and 0.150 mm voxel size. The DICOM (digital imaging and communications in medicine) files were exported. On the same day (T*), an IOS of the maxilla arch was performed with TRIOS scanner (3SHAPE, Copenhagen, Denmark) and the Standard Tessellation Language (STL) file was exported. These two acquisitions were used to digitally design and manufacture the personalized lingual device.

The orthodontic treatment started 14 days later (T0). A new IOS of the maxilla arch was done on this day and at every appointment of the patient (every four to five weeks). This resulted in the export of *n* STL files of the maxillary teeth crowns in high resolution, which were used to create the initial and intermediate models.

Once the retraction of the canines was clinically acceptable, the lingual mechanism was removed. A CBCT scan of the maxilla was acquired using the same unit and the same settings as the first one. The study then stopped, and the orthodontic treatment of the patient was carried on with vestibular braces.

2.3. 3D reconstruction of initial (T0) model

The segmentation of the initial CBCT scan was performed by a trained operator using Mimics Innovation Suite software (version 17 Research edition, Materialise, Leuven, Belgium). A semi-automated process was followed in accordance with best practice usage, by thresholding the main elements (maxilla and teeth) and manually refining the missing parts and artifacts. The maxillary bone and the teeth were individually isolated into different elements (see Figure 2, top-left panel) and, for each of them, 3D surface parts were exported in STL files. At this step, the periodontal ligament was not modeled.

For the following steps of the study, detailed anatomy of the posterior teeth crowns (premolars and molars) was needed. This anatomy could not be retrieved from the CBCT scan, due to the resolution of the acquisition and to artifacts caused by metallic restorations (Baan et al., 2021; de Waard et al., 2016). To get a surface model with precise anatomy of posterior teeth crowns, Geomagic Studio software (version 2012, Geomagic, Rock Hill, USA) was used to fuse the result of the segmentation of the initial CBCT and T0 IOS (no clinical changes were found between superimposed T* and T0 IOS which were taken 14 days apart, see Figure S1). In order to align the IOS with the segmentation, we used an Iterative Closest Point algorithm (ICP) (Besl and McKay, 1992) localized on the posterior teeth crowns ("Best Fit Alignment" in Geomagic software). ICP registration is a reliable and frequently used method for alignment of similar surfaces (Baan et al., 2021; de Waard et al., 2016; O'Toole et al., 2019). This process is illustrated in Figure 2 and detailed in the Supplementary Materials, Section B.

2.4. 3D reconstruction of intermediate (T1 to Tn) models

To reconstruct the intermediate 3D models (named T1 to Tn), Geomagic Studio software was used to reposition the segmented canines of the T0 model on the canines' crowns of the intermediate IOS.

To align the IOS on the model, we used the same process of ICP alignment ("Best Fit Alignment" in Geomagic software) localized on the crowns of the premolars and molars, considered as stable references. These "Best Fit Alignments" of several IOS using a reference structure have been shown to be highly reliable (O'Toole et al., 2019). Then, we used a second ICP alignment localized on the canine crowns to align the segmented canines (T0 model) with the intermediate position of the canines. Since the segmented teeth contained their roots, we were able to precisely track the position of the canines in the

maxilla at any time of the study. This process is illustrated in Figure 3 and detailed in the Supplementary Materials, Section B.

2.5. Validation of the tracking protocol

To validate our intermediate model reconstruction, a CBCT was used to retrieve the final position of the canines. This final position was compared to the position of canines from the last intermediate model (Tn).

First, the final CBCT was aligned with the initial CBCT using a local 3D voxel-based superimposition taking the maxillary bones as stable structures (Dot et al., 2020). To this aim, we used the open-source software ITK-SNAP (version 3.6.0; www.itksnap.org) (Yushkevich et al., 2006) and 3D Slicer (version 4.7.0; www.slicer.org) (Fedorov et al., 2012), following Dental and Craniofacial Bionetwork for Image Analysis (DCBIA) method (Ruellas et al., 2016).

Once the final CBCT was aligned with the initial one, it was imported in Mimics software to retrieve the segmented models of the canines at the end of the study. Rigid body displacements between the position of canines in the Tn model with these latter segmented canines were calculated.

2.6. Evaluation of clinical results

The displacement of the canines was evaluated both qualitatively and quantitatively using 3D Slicer software. We performed visualization via the “Model To Model Distance” and “Shape Population Viewer” modules of the SlicerSALT project (salt.slicer.org) (Vicory et al., 2018).

The global rigid body displacements of the canines’ centroids were calculated. Rigid body translation components were calculated along the x, y and z axis. Euler extrinsic angles were calculated based on a right-handed orthogonal basis centered on the centroid of the canines,

with the z axis pointing towards the apex of the teeth, the y axis towards their distal side and the x axis orthogonal to the yz plane. The order of the rotations was x, y', z''.

2.7. Finite element analysis

A preliminary FEM was developed to underpin the relevance of our tracking protocol in supporting FEA. Only the key points of the FEM are outlined here. More details are given in the Supplementary Materials, Section C.

In order to reduce the computational time, part of the T0 model was used to set up the geometry of the FEM which included the trans-canine arch, the two canines, their periodontal ligament (PDL) and part of the maxillary bone (Figure 4). The two bone parts were extracted from the whole maxilla by making virtual cuts far enough from the studied teeth, and their displacement was restricted (Figure S4). The personalized orthodontic device designed for this study allowed an accurate description of the point of application and orientation of the orthodontic forces in the FEM (Figure S4). Their magnitude was set to 100 cN according to clinical data.

Maxillary structures are heterogeneous and exhibit an anisotropic, nonlinear behavior. As our goal was to show the relevance of our 3D tracking protocol to support FEA, we were not concerned with detailed constitutive modeling. Thus, as a first step and for illustration purposes, we used simplified constitutive models for all the structures of the FEM. Teeth were considered as rigid bodies. The lingual device and the PDL were modeled as linearly elastic materials. In order to allow for irreversible OTM, bone was modeled through a Zener model (Figure S5), whose constitutive law reads:

$$\sigma = \sigma_e + \sigma_v, \qquad \sigma_e = \mathbb{C}\,\varepsilon_e, \qquad \sigma_v = 2\,\eta\,\dot{\gamma}_v,$$

where σ is the stress tensor, additively split into an elastic stress σ_e—related to the elastic strain ε_e through the elastic tensor $\mathbb{C}$— and a (deviatoric) viscous stress σ_v—related to the (deviatoric) viscous strain rate $\dot{\gamma}_v$ through the viscosity coefficient η, the latter being related to the characteristic time τ of the OTM. This parameter is strongly patient-specific: patient's

age and health state, biological activity, bone microstructure—just to mention a few—may affect the value of . Moreover, as the mechanobiological response of bone is likely nonlinear, it should not be expected to be a constant.

All the elastic coefficients were fixed according to relevant literature. Thus, overall, only one free material parameter was left, *i.e.* the characteristic time τ, that was calibrated against clinical data (models T0 to Tn). Comparison between clinical and numerical results was performed with respect to the rigid body translations and Euler extrinsic angles of the canines.

3. RESULTS

3.1. Clinical results and surface models

The retraction treatment lasted 7 months. Figure 5 shows the clinical calendar and the associate data acquisition. Starting from T0, a total of 8 IOS were acquired, leading to models T0 (initial model) to T7 (final model).

3.2. Validation of the tracking protocol

A qualitative evaluation of the 3D voxel-based superimposition of initial and final CBCT visually showed no displacement of maxillary premolars and molars (Figure 6 and Supplementary movie SM1). This confirmed the possibility of using these teeth as stable structures for the construction of the intermediate models. Incisors teeth and especially left lateral incisor showed a small displacement with a spontaneous resolution of a few millimeters of their crowding, probably due to the space created by the recoil of the canines. These observations justified the assumption to have considered only the maxillary bone around the canines in this study.

The differences in positions of the canines in the T7 model and in the final CBCT were quantified by the rigid body displacements between the two models, computed through Geomagic Studio software (Table ST1 of Supplementary Materials). These displacements were less than 0.2 mm in translation and less than 1° in rotation. They were clinically acceptable and within the actual spatial resolution of CBCT. These results validated the proposed tracking protocol and our process of reconstruction of intermediate models.

3.3. Evaluation of clinical results

Figure 7 shows the displacement fields of the right and left canines in models T3, T5, and T7, taking T0 as reference. Colors refer to the magnitude of the displacement. At T7, the range of values [minimal – maximal] taken by the magnitude of the displacement field was [2.4 - 5.6 mm] for the right canine, and [2.2 - 6.2 mm] for the left one. The higher displacement was found at the tip of the cusps, and a slight intrusion (around 2 mm) was observed at the apex. The measured rigid body displacements of the canines (translations and Euler angles in the x, y', z'' order, referred to the canine centroids) from step T0 to T1 through T7 are reported in Figure 8 and in Table ST2 of Supplementary Materials.

3.4. Finite Elements Analysis

Clinical data obtained from models T0 to T7 were used to calibrate the free parameter of our FEM, i.e. the OTM characteristic time τ. To this aim, we performed a parametric analysis searching for the values of τ best matching the clinical data. A preliminary observation of clinical data revealed two main features. First, the OTM in the direction of the applied loads is much larger than in the other directions. Secondly, OTM is characterized by two time scales, being slower during the first half of the treatment. Therefore, for the sake of simplicity, the identification of the characteristic time τ was performed only with respect to the translation of the canines in the y direction and separately in the two phases of the treatment. A good match was found by taking τ = 0.12 hours between T0 and T4, then τ = 0.06 hours between

T4 and T7. Simulated displacements (translations and rotations) of both right and left canines showed a good agreement with the corresponding clinical data, with exception of the translations along z axis. Rotations around the x axis were also slightly overestimated by the numerical model. The simulated rigid body displacements of the canines (referred to the canine centroids) from step T0 to T1 through T7 are reported in Figure 8 and in Table ST2 of Supplementary Materials.

A qualitative assessment of the simulation results can be made using transparent overlays of the clinical canine models over the simulation models. As showed in Figure 9, the simulated teeth showed a movement of rotation around their apex, in accordance to the clinical data. The clinical displacement that was not simulated correctly was the intrusion of the teeth.

4. DISCUSSION

4.1. Tracking 3D orthodontic tooth movement

The main goal of this paper was to propose a protocol to effectively track the 3D orthodontic movement of the canines. Our method of tooth movement tracking, using only one acquisition with ionizing radiation, proved to be effective and showed a clinically acceptable error. The ability to track teeth and roots displacements is clinically appealing, and the possibility to do so with a low ionizing radiation dose is a main asset (Lee et al., 2015, 2014).

We tested our protocol by tracking the 3D OTM of a patient undergoing canine retraction over a seven-month period. Intermediate models of the canines were generated monthly at each clinical appointment. The efficiency of our process of reconstruction of intermediate models was checked by a second CBCT scan at the end of the study. Being used only for validation purposes, the second CBCT scan shall not be included in the clinical protocol. This final validation shows the clinical transfer potential of this technique, and had not been performed previously (Likitmongkolsakul et al., 2018). Our new protocol represents an

294 improvement of a technique previously described by our team (Bouton et al., 2017). Our new
295 technique is more accurate and automatized as it uses an ICP algorithm and can be applied
296 to a much longer treatment.
297
298 ### *4.2. Supporting FEA*
299 FEA has a great potential to improve quality and efficiency of orthodontic treatments, but for
300 now there is no prospective model of human OTM. The main issue is the availability of
301 reliable clinical data to calibrate and validate the models. Our new protocol can usefully
302 support FEA of OTM. We illustrated this point by developing a preliminary, patient-specific
303 FEM to simulate the seven-month canine retraction of a patient. Clinical data were used to
304 calibrate the OTM characteristic time τ in the FEA. Calibration was eased by the
305 personalized orthodontic device designed for this study, delivering a statically determinate
306 system of forces. Other orthodontic devices could be used but this may introduce uncertainty
307 in the calibration process. Calibration was performed with respect to the main orthodontic
308 displacement, i.e. the canine retraction in the occlusal plane (y direction). The numerical
309 model was able to reproduce the latter with excellent accuracy. However, translation along z
310 axis did not match the clinical intrusion movement, which suggests that this movement might
311 be due to functional forces (i.e. occlusal or muscular forces) not simulated in our study.
312 Moreover, the value of τ was observed to change somewhere between T4 and T5. This
313 might be due to a change of the occlusal forces or of the biological activity but the source of
314 this effect remains unclear (de Gouyon Matignon de Pontouraude et al., 2021). These
315 difficulties underline the relevance of clinical data to support the development of reliable
316 FEM.
317
318 ### *4.3. Perspectives and limitations*
319 Our preliminary model could be used to explore the consequences of variations of the force
320 system and therefore provide clinical cues. For example, it is possible to assess the position

of the 3D center of resistance of the canines or to identify the line of action of the forces producing a target OTM.

This study has some limitations that may impact our goals and conclusions. These issues are briefly discussed below and will be addressed in future investigations.

1. The proposed 3D tracking procedure can be used for research purposes but a higher degree of automation shall be attained before it to be transferred to clinical practice. Indeed, our protocol requires operators trained in computer modelling and remains tedious because of the need of thorough segmentation of the CBCT image and manipulation of the 3D models to fuse the crowns of the IOS with the tooth models obtained from the segmentation. It would also be useful to test this procedure using CBCT images acquired using low dose protocols, which might hinder the segmentation process.
2. Our procedure needs stable landmarks to align the intermediate IOS on the initial model. In our study, we were able to use the posterior crowns as stable structures, as they were not included in the force system. To apply this method with more traditional orthodontic appliances, TADs or palatal rugae could be used as stable structures (Chen et al., 2011; de Gouyon Matignon de Pontouraude et al., 2021; Likitmongkolsakul et al., 2018). We could not use them in our study because these structures were not properly recorded in our IOS.
3. Canine root morphology was clear at the time the device was made and the initial center of resistance was estimated as per Fig. 1-C. However, the position of the center of resistance depends on the type of OTM (Meyer et al., 2010) and mechanical considerations should be made for each case (Kum et al., 2004). Therefore, our estimate of the center of resistance might not be accurate. This could have a relation with the tipping of the canines clinically observed, as the real position of the center of resistance of the canines was probably apical to the line of action of our forces.

4. Boundary conditions of the FEM may not be accurate. In particular, we did not include functional forces in our model. This could have a relation with the difference between clinical and numerical results in terms of intrusion/extrusion. This shows the major difficulty to obtain the full force system experienced by the teeth, undesired functional forces being sometimes non-negligible. The use of light-cured cement placed on top of molars to create a gap between upper and lower teeth might have helped to reduce undesired occlusal loading of the moving canines due to contacts with the lower teeth (Zhong et al., 2019).
5. The constitutive models of our FEM shall be improved, namely to account for the anisotropic, nonlinear response of the PDL and for the alveolar bone remodeling, as well as for the heterogeneity of maxillary structures. This question is out of the scope of this paper and will be addressed in future work. It should be mentioned that several models of bone remodeling have been proposed (Chen et al., 2014; George et al., 2019; Hamanaka et al., 2017). However, clinical data to support these models are hardly accessible and it is still challenging to obtain reliable information about mechanobiologically relevant parameters (Van Schepdael et al., 2013), bone density and micro-anatomy (Cattaneo et al., 2005), and precise periodontal ligament comportment (Uhlir et al., 2016).

Acknowledgements

The authors would like to thank Dr Jean-Paul Forestier (AP-HP) for his clinical and biomechanical advice which greatly assisted this study.

Funding

This research did not receive any specific grant from funding agencies in the public, commercial, or not-for-profit sectors.

Conflict of interest statement

None to declare.

Research Data

3D surface model files of IOS, T0 model used for the simulation and canines models (T0 to T7) are available from the authors upon request.

REFERENCES

Albogha, M.H., Takahashi, I., 2015. Generic finite element models of orthodontic mini-implants : are they reliable ? Journal of biomechanics 48, 3751–3756. https://doi.org/10.1016/j.jbiomech.2015.08.015

Baan, F., Bruggink, R., Nijsink, J., Maal, T.J.J., Ongkosuwito, E.M., 2021. Fusion of intra-oral scans in cone-beam computed tomography scans. Clin Oral Invest 25, 77–85. https://doi.org/10.1007/s00784-020-03336-y

Besl, P.J., McKay, N.D., 1992. A method for registration of 3-D shapes. IEEE Trans. Pattern Anal. Mach. Intell. 14, 239–256. https://doi.org/10.1109/34.121791

Bourauel, C., Vollmer, D., Jäger, A., 2000. Application of bone remodeling theories in the simulation of orthodontic tooth movements. J Orofac Orthop 61, 266–279.

Bouton, A., Simon, Y., Goussard, F., Teresi, L., Sansalone, V., 2017. New finite element study protocol : clinical simulation of orthodontic tooth movement. International orthodontics. https://doi.org/10.1016/j.ortho.2017.03.001

Burstone, C.J., 2015. Physics and clinical orthodontics : 100 years ago and today. American journal of orthodontics and dentofacial orthopedics 147, 293–294. https://doi.org/10.1016/j.ajodo.2014.12.011

Cattaneo, P.M., Dalstra, M., Melsen, B., 2005. The finite element method : a tool to study orthodontic tooth movement. Journal of dental research 84, 428–433. https://doi.org/10.1177/154405910508400506

Chen, G., Chen, S., Zhang, X.Y., Jiang, R.P., Liu, Y., Shi, F.H., Xu, T.M., 2011. Stable region for maxillary dental cast superimposition in adults, studied with the aid of stable miniscrews. Orthodontics & craniofacial research 14, 70–79. https://doi.org/10.1111/j.1601-6343.2011.01510.x

Chen, J., Li, W., Swain, M.V., Ali Darendeliler, M., Li, Q., 2014. A periodontal ligament driven remodeling algorithm for orthodontic tooth movement. Journal of biomechanics 47, 1689–1695. https://doi.org/10.1016/j.jbiomech.2014.02.030

de Gouyon Matignon de Pontouraude, M.A., Von den Hoff, J.W., Baan, F., Bruggink, R., Bloemen, M., Bronkhorst, E.M., Ongkosuwito, E.M., 2021. Highly variable rate of orthodontic tooth movement measured by a novel 3D method correlates with gingival inflammation. Clin Oral Invest 25, 1945–1952. https://doi.org/10.1007/s00784-020-03502-2

de Waard, O., Baan, F., Verhamme, L., Breuning, H., Kuijpers-Jagtman, A.M., Maal, T., 2016. A novel method for fusion of intra-oral scans and cone-beam computed tomography scans for orthognathic surgery planning. Journal of Cranio-Maxillofacial Surgery 44, 160–166. https://doi.org/10.1016/j.jcms.2015.11.017

Dot, G., Rafflenbeul, F., Salmon, B., 2020. Voxel-based superimposition of Cone Beam CT scans for orthodontic and craniofacial follow-up: Overview and clinical implementation. International Orthodontics S1761722720300991. https://doi.org/10.1016/j.ortho.2020.08.001

Fedorov, A., Beichel, R., Kalpathy-Cramer, J., Finet, J., Fillion-Robin, J.-C., Pujol, S., Bauer, C., Jennings, D., Fennessy, F., Sonka, M., Buatti, J., Aylward, S., Miller, J.V., Pieper, S., Kikinis, R., 2012. 3D Slicer as an image computing platform for the quantitative imaging network. Magnetic resonance imaging 30, 1323–1341. https://doi.org/10.1016/j.mri.2012.05.001

George, D., Wagner, D., Bolender, Y., Laheurte, P., Piotrowski, B., Didier, P., Bensidhoum, M., Herbert, V., Spingarn, C., Rémond, Y., 2019. A preliminary approach in the prediction of orthodontic bone remodeling by coupling experiments, theory and numerical models. Computer Methods in Biomechanics and Biomedical Engineering 22, S60–S61. https://doi.org/10.1080/10255842.2020.1713479

Hamanaka, R., Yamaoka, S., Anh, T.N., Tominaga, J.-Y., Koga, Y., Yoshida, N., 2017. Numeric simulation model for long-term orthodontic tooth movement with contact

boundary conditions using the finite element method. Am J Orthod Dentofacial Orthop 152, 601–612. https://doi.org/10.1016/j.ajodo.2017.03.021
Hannam, A.G., 2011. Current computational modelling trends in craniomandibular biomechanics and their clinical implications. Journal of oral rehabilitation 38, 217–234. https://doi.org/10.1111/j.1365-2842.2010.02149.x
Hasegawa, M., Adachi, T., Takano-Yamamoto, T., 2016. Computer simulation of orthodontic tooth movement using CT image-based voxel finite element models with the level set method. Computer methods in biomechanics and biomedical engineering 19, 474–483. https://doi.org/10.1080/10255842.2015.1042463
Henneman, S., Von den Hoff, J.W., Maltha, J.C., 2008. Mechanobiology of tooth movement. The european journal of orthodontics 30, 299–306. https://doi.org/10.1093/ejo/cjn020
Kapila, S.D., Nervina, J.M., 2015. CBCT in orthodontics: assessment of treatment outcomes and indications for its use. Dentomaxillofacial Radiology 44, 20140282. https://doi.org/10.1259/dmfr.20140282
Krishnan, V., Davidovitch, Z., 2009. On a path to unfolding the biological mechanisms of orthodontic tooth movement. Journal of dental research 88, 597–608. https://doi.org/10.1177/0022034509338914
Kum, M., Quick, A., Hood, J.A., Herbison, P., 2004. Moment to force ratio characteristics of three Japanese NiTi and TMA dosing loops. Aust Orthod J 20, 107–114.
Lee, R.J., Pham, J., Choy, M., Weissheimer, A., Dougherty, H.L., Sameshima, G.T., Tong, H., 2014. Monitoring of typodont root movement via crown superimposition of single cone-beam computed tomography and consecutive intraoral scans. American journal of orthodontics and dentofacial orthopedics 145, 399–409. https://doi.org/10.1016/j.ajodo.2013.12.011
Lee, R.J., Weissheimer, A., Pham, J., Go, L., de Menezes, L.M., Redmond, W.R., Loos, J.F., Sameshima, G.T., Tong, H., 2015. Three-dimensional monitoring of root movement during orthodontic treatment. American journal of orthodontics and dentofacial orthopedics 147, 132–142. https://doi.org/10.1016/j.ajodo.2014.10.010
Likitmongkolsakul, U., Smithmaitrie, P., Samruajbenjakun, B., Aksornmuang, J., 2018. Development and Validation of 3D Finite Element Models for Prediction of Orthodontic Tooth Movement. International Journal of Dentistry 2018, 1–7. https://doi.org/10.1155/2018/4927503
Marangalou, J.H., Ghalichi, F., Mirzakouchaki, B., 2009. Numerical simulation of orthodontic bone remodeling. Orthodontic waves 68, 64–71. https://doi.org/10.1016/j.odw.2008.12.002
Meyer, B.N., Chen, J., Katona, T.R., 2010. Does the center of resistance depend on the direction of tooth movement ? American journal of orthodontics and dentofacial orthopedics 137, 354–361. https://doi.org/10.1016/j.ajodo.2008.03.029
O'Toole, S., Osnes, C., Bartlett, D., Keeling, A., 2019. Investigation into the accuracy and measurement methods of sequential 3D dental scan alignment. Dental Materials 35, 495–500. https://doi.org/10.1016/j.dental.2019.01.012
Roberts, W.E., Viecilli, R.F., Chang, C., Katona, T.R., Paydar, N.H., 2015. Biology of biomechanics : finite element analysis of a statically determinate system to rotate the occlusal plane for correction of a skeletal class III open-bite malocclusion. American journal of orthodontics and dentofacial orthopedics 148, 943–955. https://doi.org/10.1016/j.ajodo.2015.10.002
Ruellas, A.C.O., Huanca Ghislanzoni, L.T., Gomes, M.R., Danesi, C., Lione, R., Nguyen, T., McNamara Jr, J.A., Cozza, P., Franchi, L., Cevidanes, L.H.S., 2016. Comparison and reproducibility of 2 regions of reference for maxillary regional registration with cone-beam computed tomography. American journal of orthodontics and dentofacial orthopedics 149, 533–542. https://doi.org/10.1016/j.ajodo.2015.09.026
Schneider, J., Geiger, M., Sander, F.-G., 2002. Numerical experiments on long-time orthodontic tooth movement. American journal of orthodontics and dentofacial orthopedics 121, 257–265. https://doi.org/10.1067/mod.2002.121007

Uhlir, R., Mayo, V., Lin, P.H., Chen, S., Lee, Y.-T., Hershey, G., Lin, F.-C., Ko, C.-C., 2016. Biomechanical characterization of the periodontal ligament : orthodontic tooth movement. The Angle orthodontist. https://doi.org/10.2319/092615-651.1

Van Schepdael, A., Vander Sloten, J., Geris, L., 2013. Mechanobiological modeling can explain orthodontic tooth movement : three case studies. Journal of biomechanics 46, 470–477. https://doi.org/10.1016/j.jbiomech.2012.10.037

Vicory, J., Pascal, L., Hernandez, P., Fishbaugh, J., Prieto, J., Mostapha, M., Huang, C., Shah, H., Hong, J., Liu, Z., Michoud, L., Fillion-Robin, J.-C., Gerig, G., Zhu, H., Pizer, S.M., Styner, M., Paniagua, B., 2018. SlicerSALT: Shape AnaLysis Toolbox, in: Reuter, M., Wachinger, C., Lombaert, H., Paniagua, B., Lüthi, M., Egger, B. (Eds.), Shape in Medical Imaging. Springer International Publishing, Cham, pp. 65–72. https://doi.org/10.1007/978-3-030-04747-4_6

Viecilli, R.F., Kar-kuri, M.H., Varriale, J., Budiman, A., Janal, M., 2013. Effects of initial stresses and time on orthodontic external root resorption. Journal of dental research 92, 346–351. https://doi.org/10.1177/0022034513480794

Wang, C., Han, J., Li, Q., Wang, L., Fan, Y., 2014. Simulation of bone remodelling in orthodontic treatment. Computer methods in biomechanics and biomedical engineering 17, 1042–1050. https://doi.org/10.1080/10255842.2012.736969

Wise, G.E., King, G.J., 2008. Mechanisms of tooth eruption and orthodontic tooth movement. Journal of dental research 87, 414–434. https://doi.org/10.1177/154405910808700509

Yushkevich, P.A., Piven, J., Hazlett, H.C., Smith, R.G., Ho, S., Gee, J.C., Gerig, G., 2006. User-guided 3D active contour segmentation of anatomical structures : significantly improved efficiency and reliability. Neuroimage 31, 1116–1128. https://doi.org/10.1016/j.neuroimage.2006.01.015

Zhong, J., Chen, J., Weinkamer, R., Darendeliler, M.A., Swain, M.V., Sue, A., Zheng, K., Li, Q., 2019. In vivo effects of different orthodontic loading on root resorption and correlation with mechanobiological stimulus in periodontal ligament. J R Soc Interface 16, 20190108. https://doi.org/10.1098/rsif.2019.0108

Figure legends

Figure 1: Individualized lingual mechanism used in this study. A: intra-oral occlusal view (see supplementary materials for details). B and C: posterior and right lateral view, respectively, of the flat portion of the trans-canine arch (CBCT segmented model), designed to be at height of the theoretical initial center of resistance of canines (in purple).

Figure 2: 3D reconstruction of initial (T0) Model. Red/blue colors: selected/unselected parts for Iterative Closest Point algorithm (ICP).

Figure 3: 3D reconstruction of the intermediate model Ti (i=1..n). Only the teeth of T0 model are shown in the upper images. Red/blue colors: selected/unselected parts for Iterative Closest Point algorithm (ICP).

Figure 4: T0 surface model after preparation for FEA with coordinate system. A. Front view with transparent bone overlay. B. Occlusal view with transparent bone overlay. C. Lateral right view.

Figure 5: Clinical calendar and data acquisition.

Figure 6: Cross-section in the axial plane of initial (greylevel) and final (red) superimposed CBCT scans. White arrows point to the left (LC) and right (RC) canines considered in this study. Their orientation indicates the point of view in Figures 7 and 9.

Figure 7: Vector fields of right (upper panel) and left (lower panel) canine displacement from situation T0 to T3, T5, and T7 (vectors at scale 1). The point of view is depicted by the white arrows in Figure 6.

Figure 8: Rigid body translations (Tx, Ty, Tz) and rotations (Rx, Ry, Rz) of right and left canine from step T0 to steps T1 through T7: comparison of clinical (“clin” labels, blue lines) and simulation (“sim” labels, orange lines) results.

Figure 9: Qualitative evaluation of canine displacement from situation T0 (plain white) to T7 clinical (blue overlay) and simulation (orange overlay). A: Right canine; B: Left canine. The points of view are depicted by the white arrows in Figure 6.

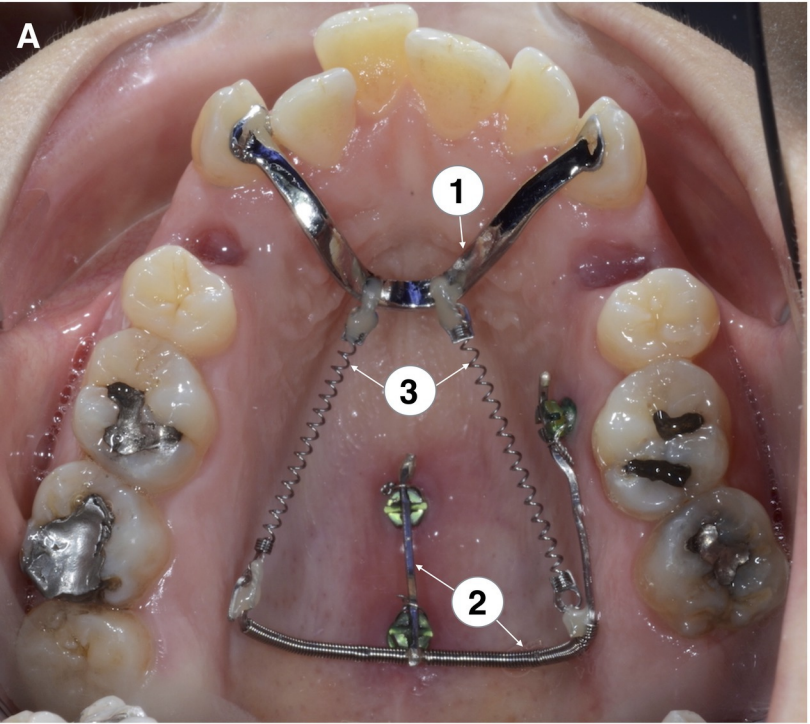
A
1
3
2

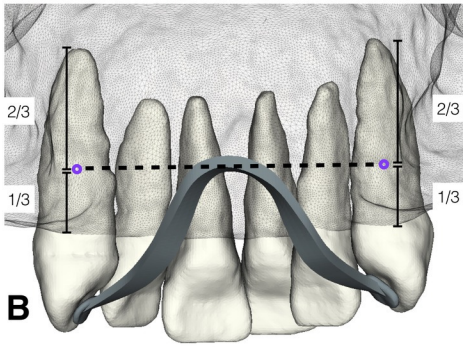
2/3
2/3
1/3
1/3
B

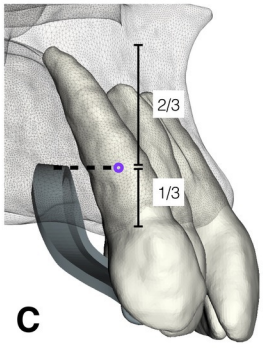
2/3
1/3
C

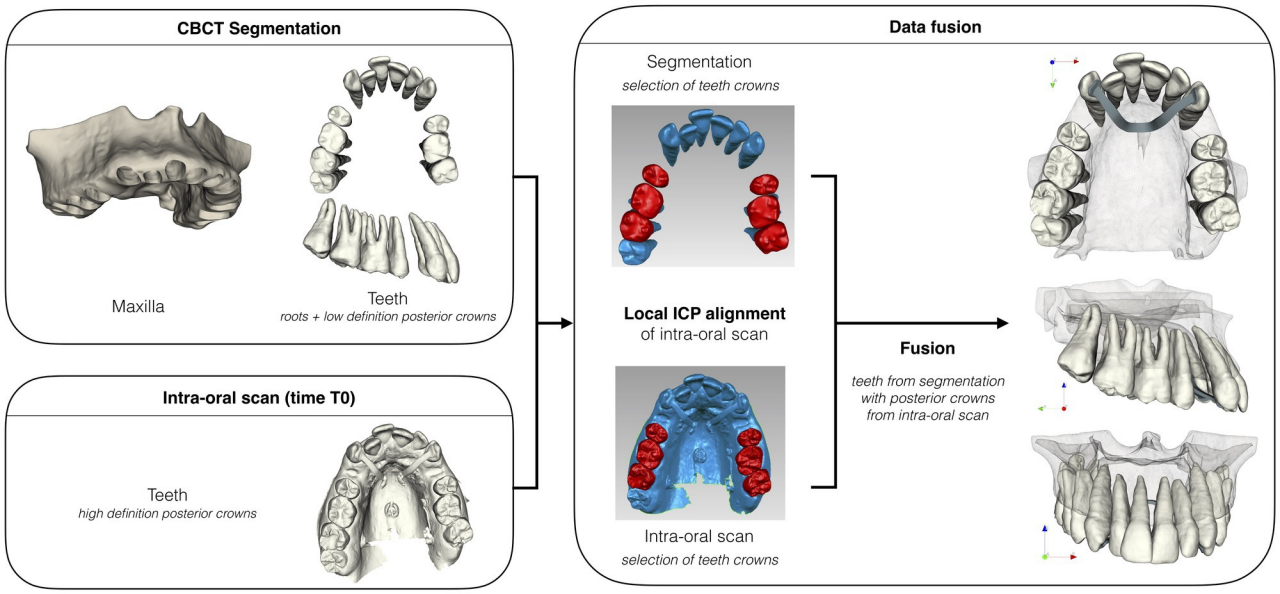
CBCT Segmentation
Maxilla
Teeth
roots + low definition posterior crowns
Intra-oral scan (time T0)
Teeth
high definition posterior crowns
Data fusion
Segmentation
selection of teeth crowns
Local ICP alignment
of intra-oral scan
Intra-oral scan
selection of teeth crowns
Fusion
teeth from segmentation
with posterior crowns
from intra-oral scan

Intermediate model 3D reconstruction

T0 Model

selection of posterior teeth crowns

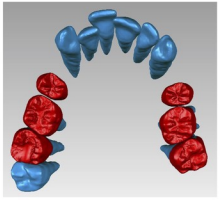

Local ICP alignment of intra-oral scan

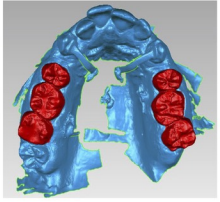

Ti intra-oral scan

selection of posterior teeth crowns

T0 Model

selection of canines crowns

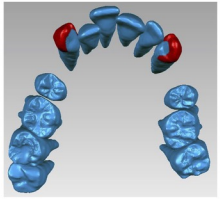

Local ICP alignment of canines

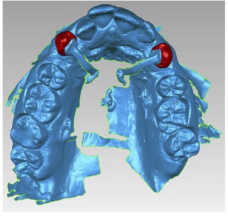

Ti intra-oral scan aligned

selection of canines crowns

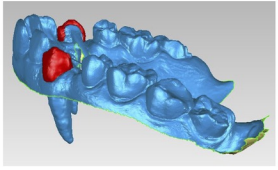

Canines aligned

canines with roots aligned on Ti intra-oral scan

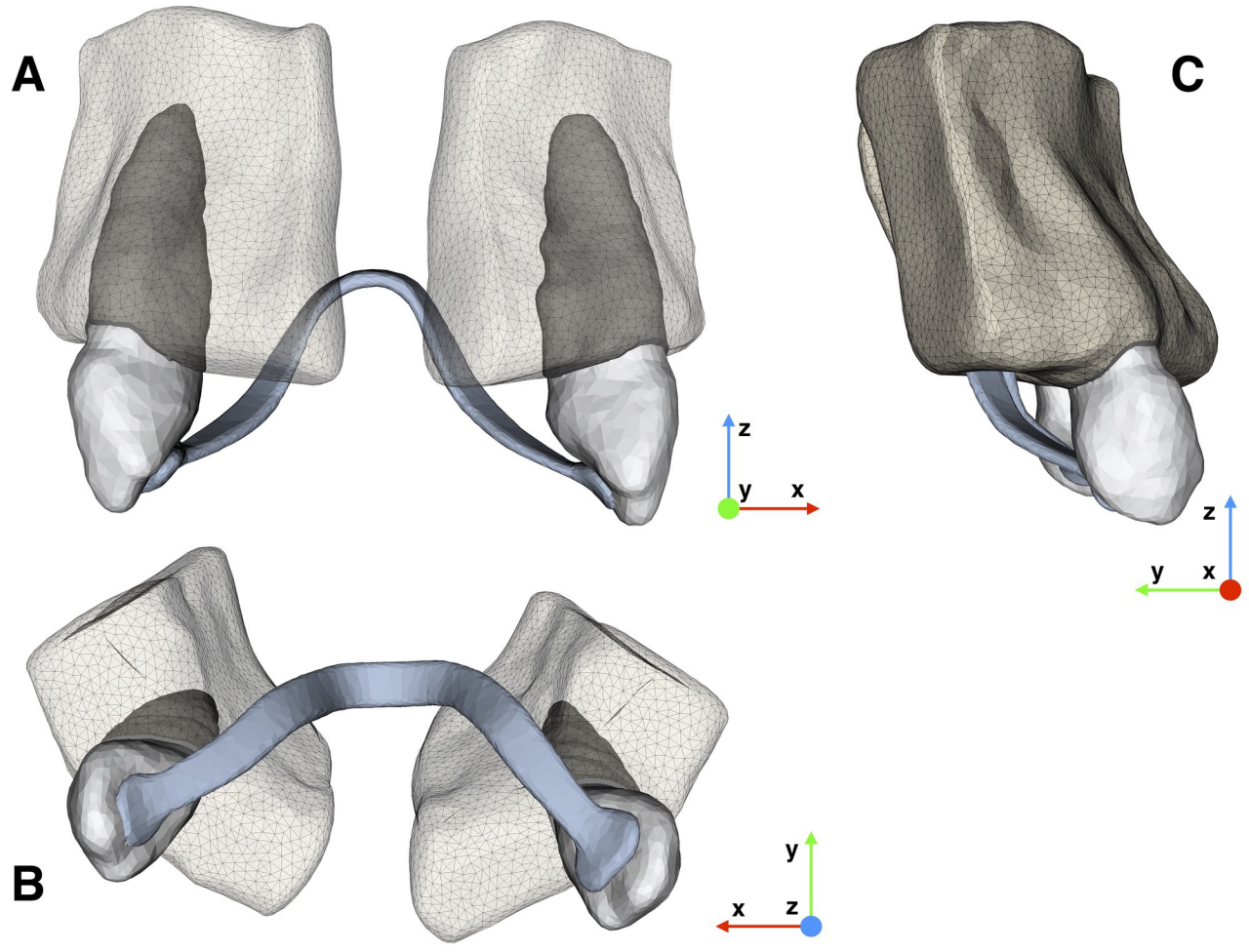
A
z
y
x
C
z
y
x
B
y
x
z

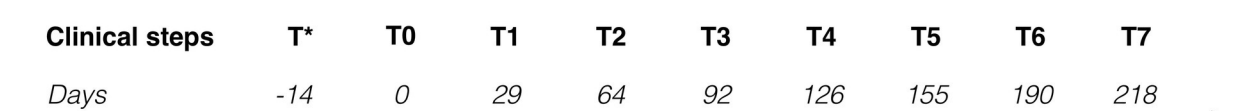
Clinical steps
T*
T0
T1
T2
T3
T4
T5
T6
T7
Days
-14
0
29
64
92
126
155
190
218
CBCT
x
x
Intra-oral scan
x
x
x
x
x
x
x
x
x

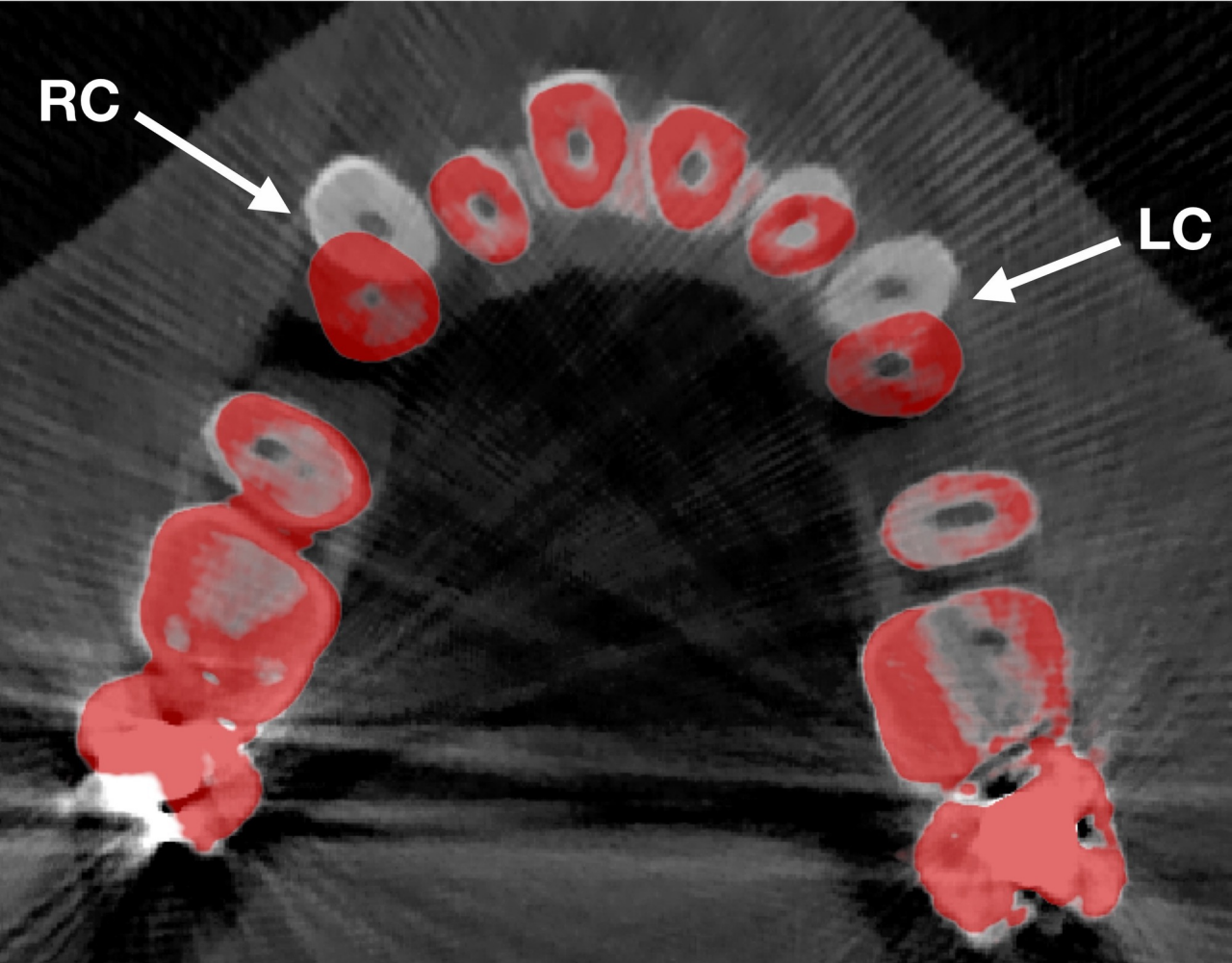
RC
LC

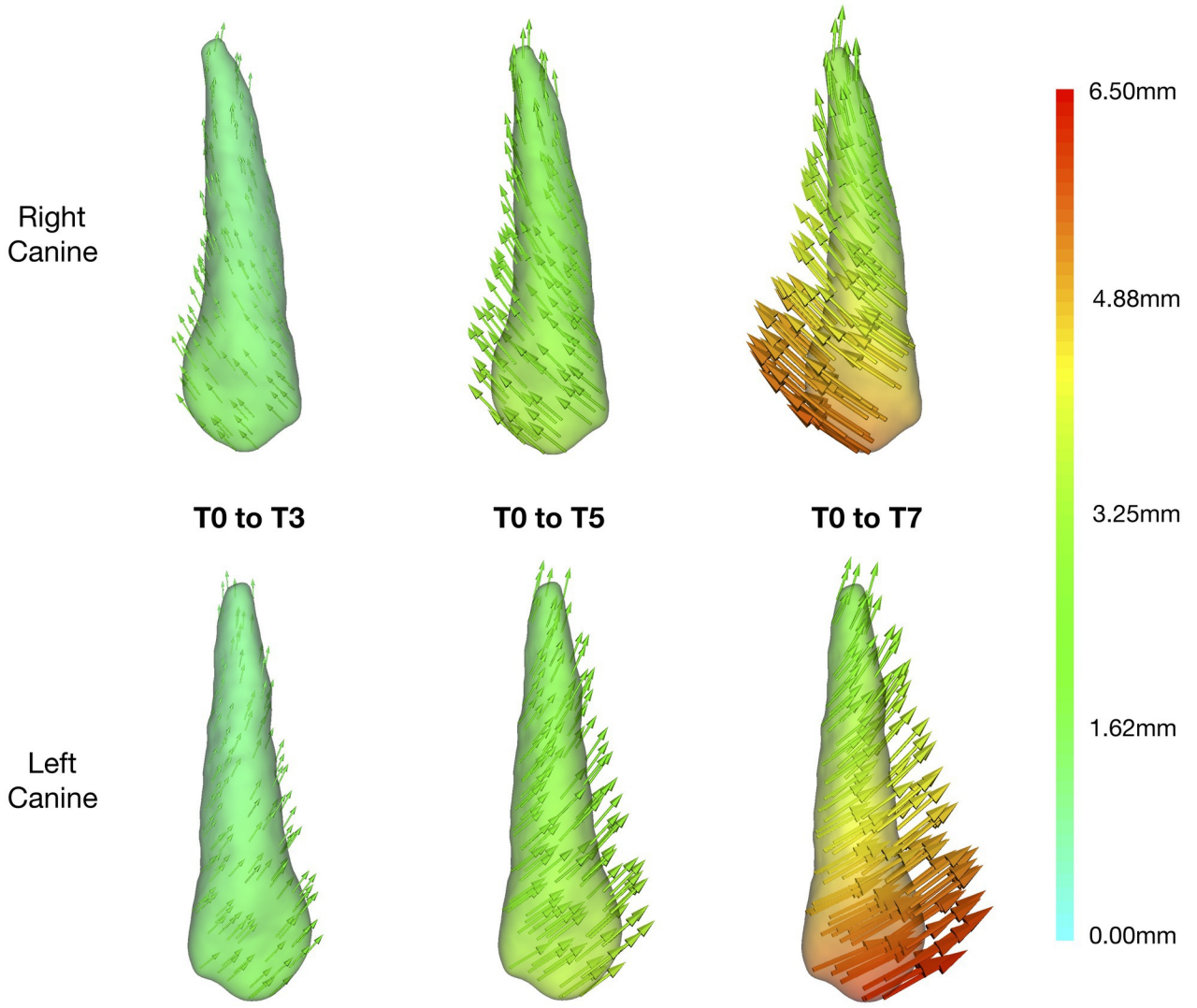
Right Canine
Left Canine
T0 to T3
T0 to T5
T0 to T7
6.50mm
4.88mm
3.25mm
1.62mm
0.00mm

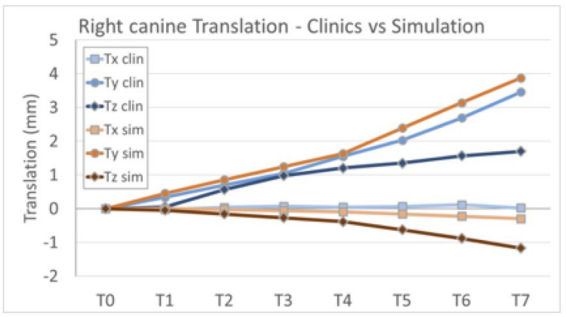
Right canine Translation - Clinics vs Simulation
Translation (mm)
Tx clin
Ty clin
Tz clin
Tx sim
Ty sim
Tz sim
5
4
3
2
1
0
-1
-2
T0
T1
T2
T3
T4
T5
T6
T7

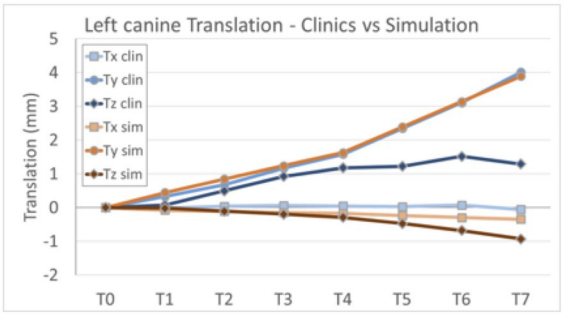
Left canine Translation - Clinics vs Simulation
Translation (mm)
Tx clin
Ty clin
Tz clin
Tx sim
Ty sim
Tz sim
5
4
3
2
1
0
-1
-2
T0
T1
T2
T3
T4
T5
T6
T7

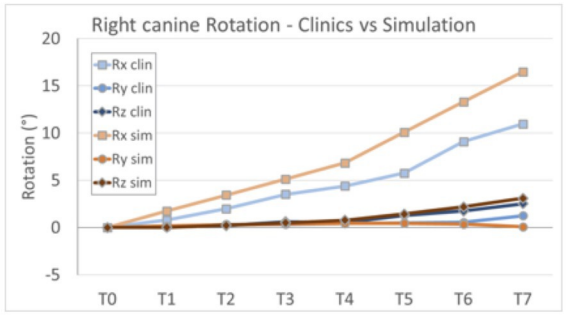
Right canine Rotation - Clinics vs Simulation
Rotation (°)
Rx clin
Ry clin
Rz clin
Rx sim
Ry sim
Rz sim
20
15
10
5
0
-5
T0
T1
T2
T3
T4
T5
T6
T7

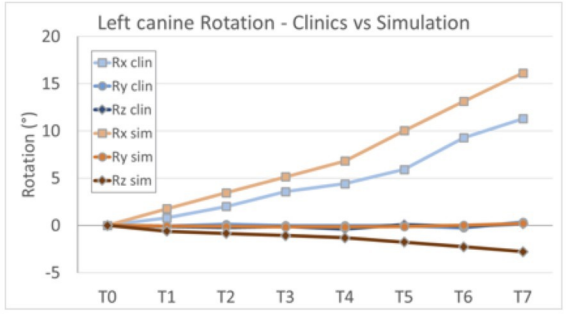
Left canine Rotation - Clinics vs Simulation
Rotation (°)
Rx clin
Ry clin
Rz clin
Rx sim
Ry sim
Rz sim
20
15
10
5
0
-5
T0
T1
T2
T3
T4
T5
T6
T7

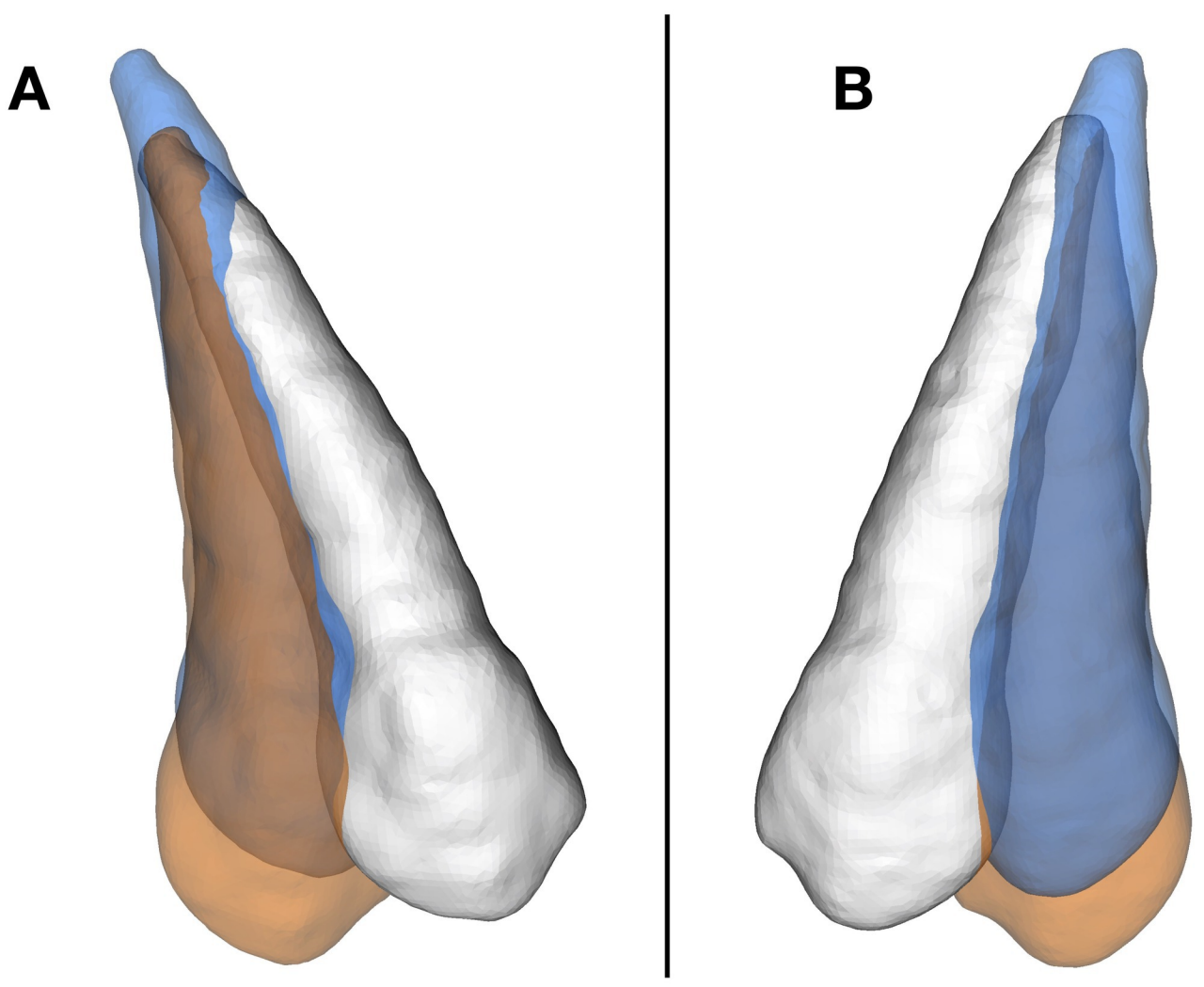
A
B

Authors, Year	*Initial model geometry*	*Updated model geometry (clinical OTM tracking)*	*Mechanical loading*	*Clinical validation of numerical results*
Bourauel et al. 2000	CAD	n/a	Theoretical loadings applied at crown level (no friction/sliding)	n/a
Schneider et al. 2002	CAD	n/a	Theoretical loadings applied at crown level (no friction/sliding)	n/a
Marangalou et al. 2009	CT-Scan (1 patient)	n/a	Theoretical loadings applied at crown level (no friction/sliding)	n/a
Wang et al. 2012	CT-Scan (1 patient)	n/a	Theoretical loadings applied at crown level (no friction/sliding)	n/a
Chen et al. 2014	CBCT scan (1 patient)	n/a	Theoretical loadings applied at crown level (no friction/sliding)	1 patient followed for 3 months
Hasegawa et al. 2016	CT-Scan (1 patient)	n/a	Theoretical loadings applied at crown level (no friction/sliding)	n/a
Hamanaka et al. 2017	µCT scan (1 dry skull)	n/a	Sliding mechanics with contact boundary conditions	n/a
Likitmongkolsakul et al. 2018	CBCT scan (2 patients)	Scanned dental models	Sliding mechanics with contact boundary conditions	2 patients followed for 4 months

OTM: Orthodontic Tooth Movement; CAD : Computer-aided design; CT : computed tomography; CBCT : cone beam computed tomography; n/a : not applicable.

Table 1. Published numerical models for long-term orthodontic tooth movement (OTM)